Electronic Supplementary Material (ESI) for Journal of Materials Chemistry A.

Supporting Information

Elucidating the Lithium Deposition Behavior in Open-Porous Copper Micro-Foam Negative Electrodes for Zero-Excess Lithium Metal Batteries

Tjark T. K. Ingber[a], Marlena M. Bela[a], Frederik Püttmann[a], Jan F. Dohmann[a], Peter Bieker[b], Markus Börner[a], Martin Winter[a,b], Marian C. Stan[b]

[a] MEET Battery Research Center, University of Münster, Corrensstraße 46, 48149 Münster, Germany

[b] Helmholtz Institute Münster (HI MS), IEK-12, Forschungszentrum Jülich GmbH, Corrensstraße 46, 48149 Münster, Germany

Corresponding author: Marian C. Stan, m.stan@fz-juelich.de

Table S1. Key parameters used for the calculation of specific energy and energy density values for Li metal batteries using NCA-based positive electrodes, Celgard 2320 polypropylene monolayer separators, an organic carbonate-based electrolyte, and negative electrodes composed of a Cu foil current collector beneath either Li metal or a Cu micro-foam, or with no additional layer on top. Electrolyte amount calculated to wet separator and fill Cu micro-foam pores (if present). Calculation adapted from Schmuch et al..[1]

Parameter	Value	Unit
Positive electrode thickness	50	µm
Positive electrode areal mass (incl. electrolyte)	16.640	mg cm^{-2}
Positive electrode areal capacity	2.820	mAh cm^{-2}
Positive electrode Al current collector thickness	6	µm
Positive electrode Al current collector mass	1.620	mg cm^{-2}
Separator + electrolyte thickness	20	µm
Separator + electrolyte mass	2.095	mg cm^{-2}
Electrolyte amount (Cu foil)	0.78	µL cm^{-2}
Electrolyte amount (52.2 µm thick Cu micro-foam)	4.50	µL cm^{-2}
Electrolyte amount (15 µm thin Cu micro-foam)	1.85	µL cm^{-2}
Negative electrode Cu current collector thickness	5	µm
Negative electrode Cu current collector mass	4.480	mg cm^{-2}
Cu micro-foam density (incl. pore space)	2.424	g cm^{-3}
Nominal cell voltage	3.7	V

Table S2. Comparison of the capacity retention values achieved in ZELMB systems with optimized Cu-based negative electrode substrates as reported in several recent studies. 3D structured negative electrode substrates are marked as *(3D)*. Voltage = upper cutoff voltage used for charge/discharge cycling. PE = positive electrode.

Negative Electrode	Positive Electrode	Electrolyte	Voltage (V)	PE mass loading (mg cm^{-2})	Reported Capacity retention	Source
Sn@Cu	NCA	1 M $LiPF_6$ in FEC/EMC 1:4 (wt.)	4.2	5	31% after 50 cycles	[2]
PEO@Cu	LFP	1 M LiTFSI in DME/DOL 1:1 (v/v) + 2 wt% $LiNO_3$	3.8	4.5	50% after 100 cycles	[3]
C/$LiNO_3$ foam@Cu *(3D)*	LFP	1 M $LiPF_6$ + 0.02 M $LiNO_3$ + 5 wt% VC in EC/DMC 1:1 (v/v)	4.0	11	49% after 100 cycles	[4]
Graphene@Cu	LFP	1 M LiTFSI in DME/DOL 1:1 (v/v) + 2 wt% $LiNO_3$	3.8	12	61% after 100 cycles	[5]

(Ga/In/Sn)@Cu	NMC 811	6 M LiFSI in DME	4.3	25	84% after 50 cycles	[6]
Surface-structured Cu	LFP	1 M LiFSI in DME	4.0	11	22% after 40 cycles	[7]
(Ga/In/Sn)@Cu	NMC 111	1 M $LiPF_6$ in FEC/DMC 1:1 (v/v)	4.3	23	38% after 40 cycles	[8]
Si-PAN@Cu	LNMO	4.5M LiFSI in $Py_{13}FSI$ + 1 wt% LiTFSI	4.85	10	80% after 120 cycles	[9]
Au@Cu mesh *(3D)*	LFP	2 M LiTFSI in DOL:DME 1:1 + 2 wt% $LiNO_3$	3.8	1	43% after 100 cycles	[10]
Cu_2O@Cu	LFP	1 M LiTFSI in DME/DOL 1:1 (v/v) + 2 wt% $LiNO_3$	3.8	22	62% after 100 cycles	[11]
Cu micro-foam *(3D)*	NCA	1 M LiDFOB + 0.2 M $LiBF_4$ in FEC:DEC (1:2)	4.2	5	47% after 50 cycles	**This work**

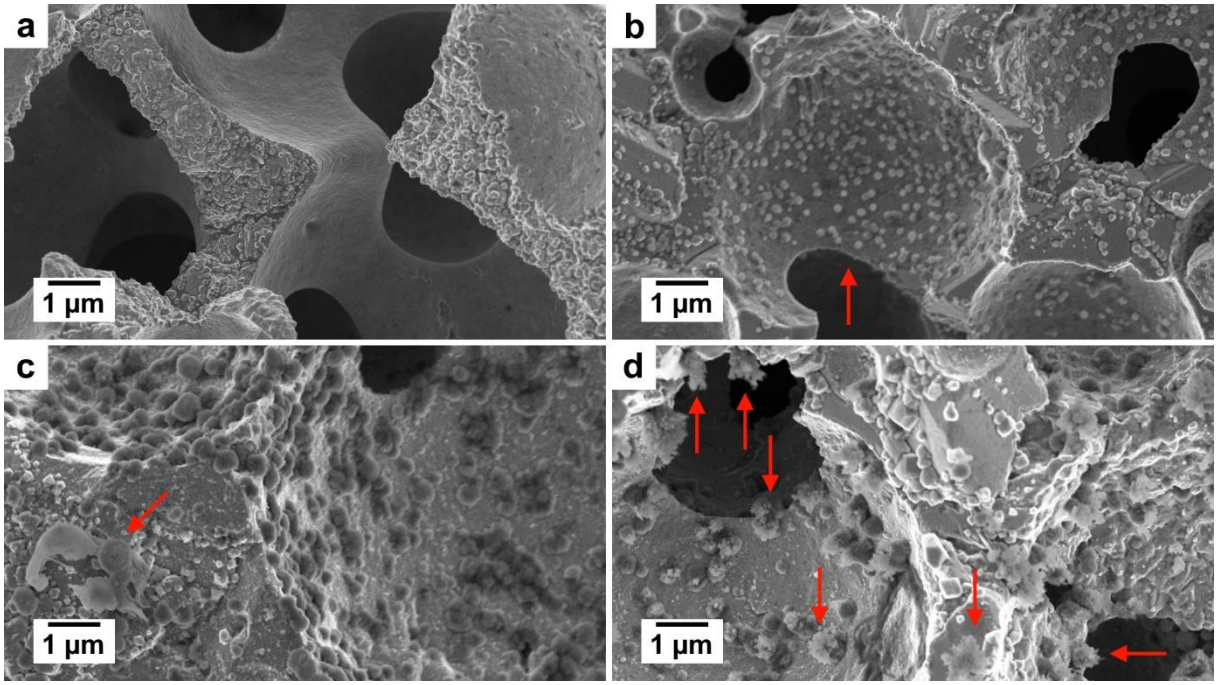

Figure S1. (a) Pristine Cu micro-foam reference and (b-d) Li nuclei covering the surfaces of the Cu micro-foam material after deposition of metallic Li corresponding to (b) 0.05 mAh cm^{-2}, (c) 0.20 mAh cm^{-2}, and (d) 1.00 mAh cm^{-2} (current density 0.1 mA cm^{-2}). Red arrows indicate (b) area with individual Li nuclei, (c) an expanding Li cluster formed from the merging of several Li deposition nuclei, and (d) mossy Li protrusions grown on the original spherical deposition nuclei.

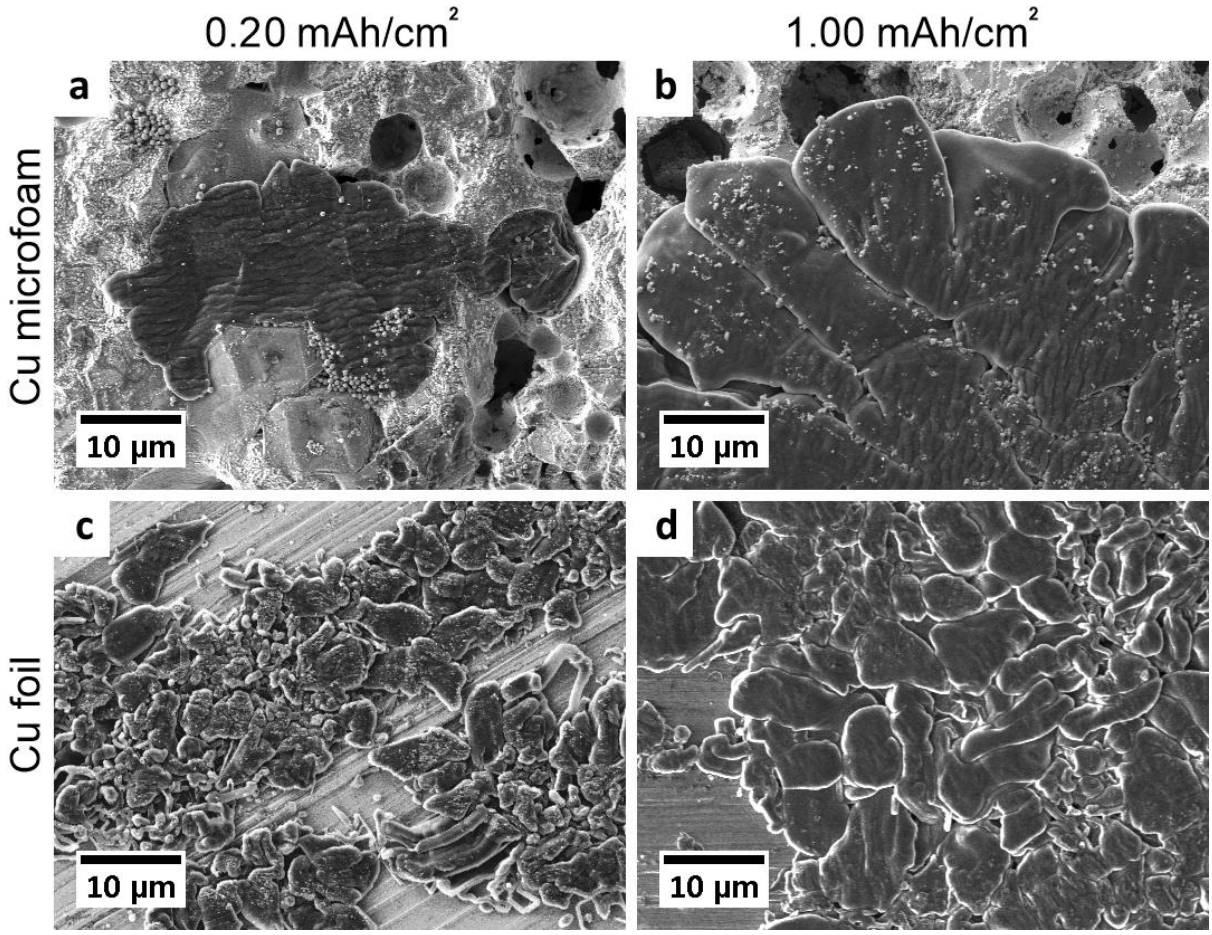

Figure S2. Enlarged top-view images of metallic bulk Li deposited on (a,b) Cu micro-foams and (c,d) plain Cu foil. Using a current density of 0.1 mA cm^{-2}, Li amounts equal to (a,c) 0.20 mAh cm^{-2} and (b,d) 1.00 mAh cm^{-2} were deposited.

In Figure 3a, a layer of a flaky material can be seen on the walls of some sub-surface pores as well as on parts of the Li structures that protrude into these pores. Figure S3 illustrates that this coating is made up of Cu from the Cu micro-foam skeleton that is redeposited during the FIB milling process. Therefore, this phenomenon can be classified as a processing artifact. Apart from this, both the top surfaces of the Li deposits and the pore walls show small Li nuclei partly covered with SEI and redeposited Cu (see Figure S1b).

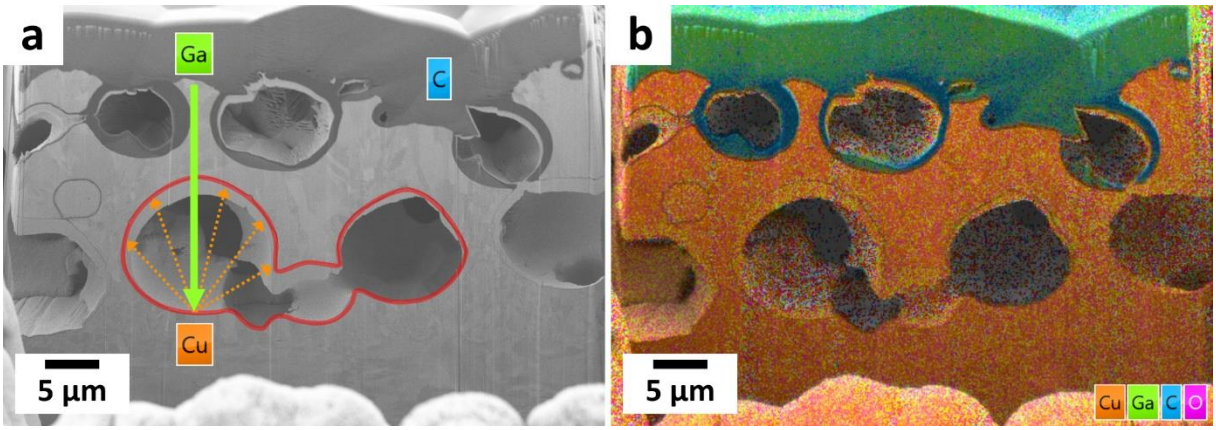

Figure S3. (a) Cross-section view of a Cu micro-foam with a protective C coating applied prior to FIB milling. The image shows a schematic representation of how Cu can be abraded and redeposited onto the pore walls (red) by the incident Ga beam used for FIB milling. (b) EDX mapping image of the same cross-section proving that the material redeposited on the pore walls is actually Cu. Color code: Cu = orange, Ga = green, C = blue, O = purple.

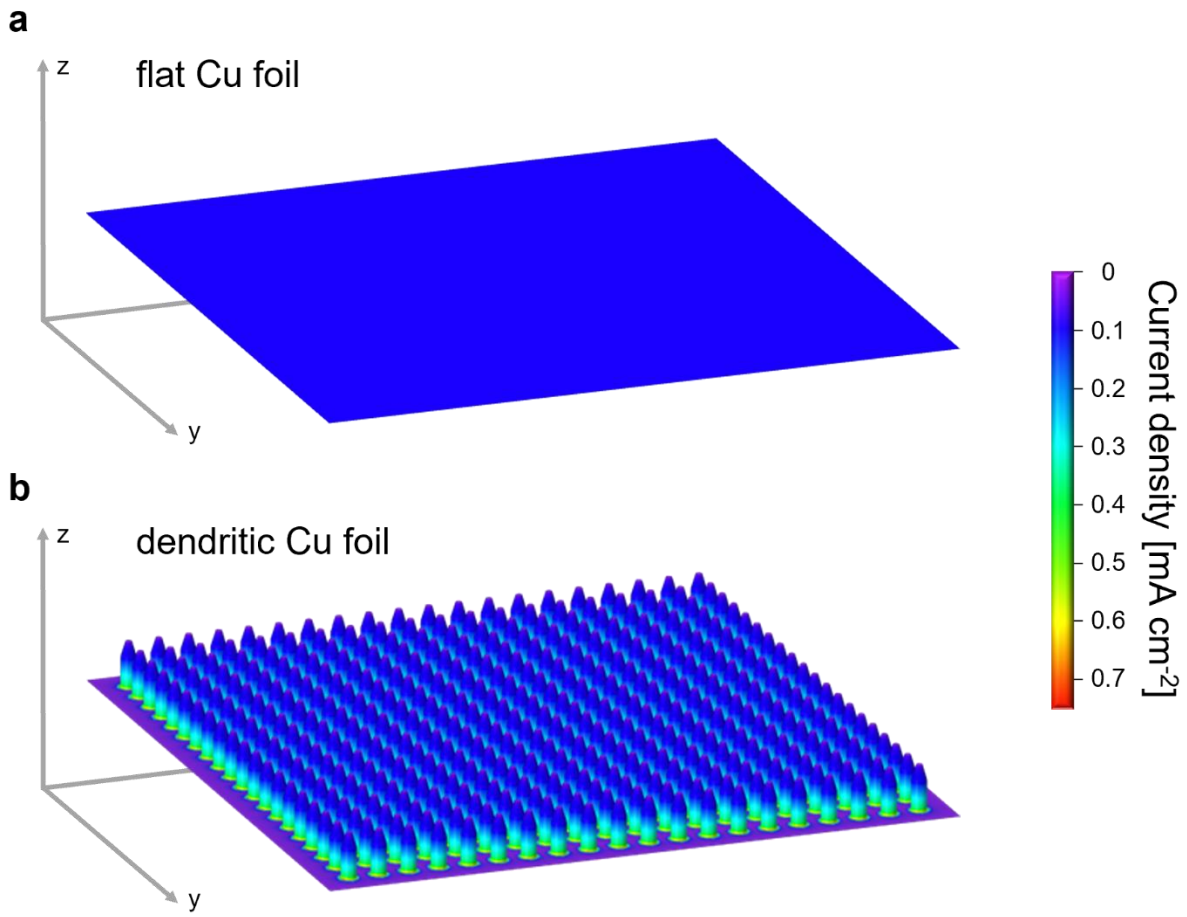

Figure S4. Current density distribution in (a) flat Cu foil and (b) a simplified model of the used dendritic Cu foil simulated with COMSOL Multiphysics. An equal current of 0.1 mA cm^{-2} relative to the geometric area in the x-y-plane was applied to both models. The same color scale was used for both current density visualizations.

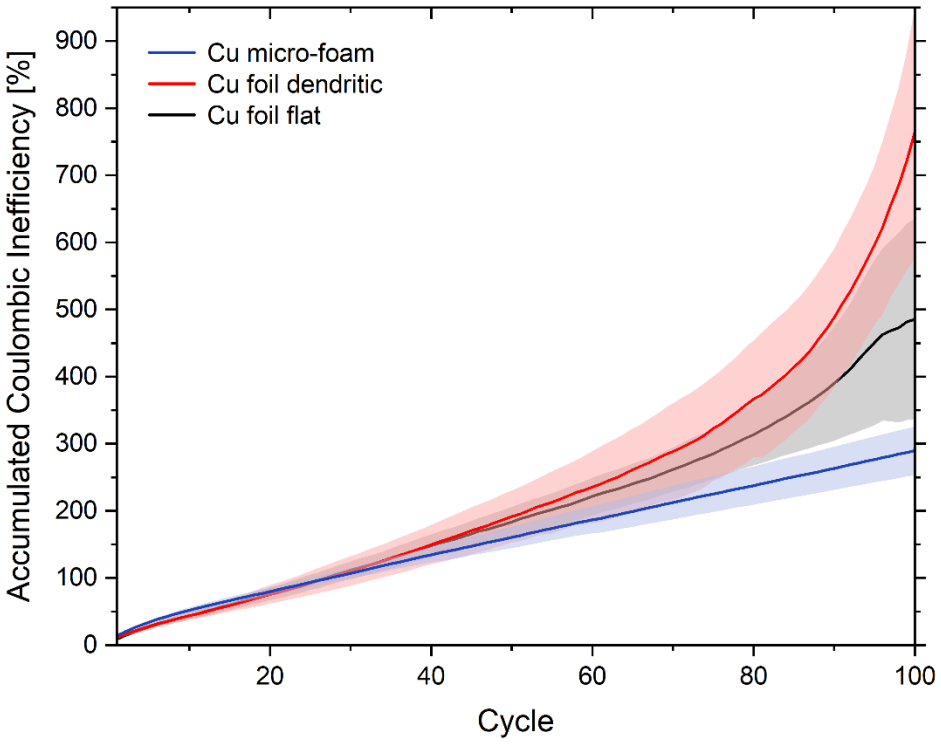

Figure S5. Accumulated Coulombic inefficiency resulting from charge/discharge cycling of NCA || Cu micro-foam (blue), NCA || Cu foil dendritic (red), and NCA || Cu foil flat (black) cells with a current density of 0.2 mA cm^{-2} (0.2 C) for 100 cycles at 40 °C. The Accumulated Coulombic inefficiency is calculated by adding up all the individual Coulombic Inefficiency values of each cycle.

References

[1] R. Schmuch, R. Wagner, G. Hörpel, T. Placke, M. Winter, *Nat. Energy* **2018**, *3*, 267.

[2] S. S. Zhang, X. Fan, C. Wang, *Electrochim. Acta* **2017**, *258*, 1201.

[3] A. A. Assegie, J.-H. Cheng, L.-M. Kuo, W.-N. Su, B.-J. Hwang, *Nanoscale* **2018**, *10*, 6125.

[4] H. Liu, X. Yue, X. Xing, Q. Yan, J. Huang, V. Petrova, H. Zhou, P. Liu, *Energy Storage Mater.* **2019**, *16*, 505.

[5] A. A. Assegie, C.-C. Chung, M.-C. Tsai, W.-N. Su, C.-W. Chen, B.-J. Hwang, *Nanoscale* **2019**, *11*, 2710.

[6] L. Lin, L. Suo, Y. Hu, H. Li, X. Huang, L. Chen, *Adv. Energy Mater.* **2021**, *11*, 2003709.

[7] J. Jung, J. Y. Kim, I. J. Kim, H. Kwon, G. Kim, G. Doo, W. Jo, H.-T. Jung, H.-T. Kim, *J. Mater. Chem. A* **2022**, *10*, 20984.

[8] S. Koul, Y. Morita, F. Fujisaki, H. Ogasa, Y. Fujiwara, A. Kushima, *J. Electrochem. Soc.* **2022**, *169*, 20542.

[9] P. Liang, H. Sun, C.-L. Huang, G. Zhu, H.-C. Tai, J. Li, F. Wang, Y. Wang, C.-J. Huang, S.-K. Jiang, M.-C. Lin, Y.-Y. Li, B.-J. Hwang, C.-A. Wang, H. Dai, *Adv. Mater.* **2022**, *34*, e2207361.

[10] E. Kim, W. Choi, S. Ryu, Y. Yun, S. Jo, J. Yoo, *J. Alloys Compd.* **2023**, 171393.

[11] J. Chen, L. Dai, P. Hu, Z. Li, *Molecules* **2023**, *28*.